# Behavior of rays near singularities in anisotropic media

V. Vavryčuk*
*Geophysical Institute, Academy of Sciences of the Czech Republic, Bočnı́ II/1401, 141 31 Praha 4, Czech Republic*
(Received 7 May 2002; published 27 February 2003)

The ray field can display a complicated pattern near singularities (acoustic axes) in inhomogeneous anisotropic elastic media. The peculiarities in the ray field arise particularly near conical and wedge singularities, which generate linear, circular, or elliptical anticaustics in their vicinities. The anticaustics represent barriers for rays and prevent the rays from crossing them. If the rays approach the anticaustic, they can be strongly curved and deflected from their original direction. The rays outside the anticaustic are forced to move around the anticaustic. The rays inside the anticaustic are captured and forced to pass the caustic generated by the singularity.

DOI: 10.1103/PhysRevB.67.054105 PACS number(s): 46.40.Cd, 62.30.+d

## I. INTRODUCTION

Singularities (also called acoustic axes or degeneracies) are directions in anisotropic media in which two or three waves have coincident phase velocities.[1–7] These directions are extremely important because they can cause anomalies in the field of polarization vectors[8,9] and in the geometry of the slowness and wave surfaces.[10,11] For example, the Gaussian curvature of the slowness surface can be infinite or it may not even be defined in the singularity.[12,13] Singularities are usually connected with the presence of caustics.[14–17] The caustics complicate the geometry of rays, but do not pose complications in ray-tracing equations. However, singularities often cause trouble in tracing rays. Since the medium is degenerate in singularities, the standard ray-tracing equations in anisotropic media[18–22] produce numerical instabilities, or they even fail whenever the ray approaches near-singularity directions.[23] So far these complications have not allowed the geometry of rays in these directions to be studied; hence little is known about the behavior of rays under anisotropy with singularities. In this paper, the behavior of rays near singularities in inhomogeneous anisotropic elastic media is studied by numerical modeling. The ray-tracing algorithm developed by Vavryčuk[24] is applied. The algorithm is a modification of the ray tracing based on evaluating the right-hand sides of equations using the polarization vectors of the traced wave. The algorithm is numerically stable and yields correct results when tracing rays in anisotropic media with all kinds of singularities. This enables us to address particularly the following points: Can a ray touch or cross the singularity? Is the geometry of the ray field affected by the singularity? How do the ray fields for various kinds of singularities differ? Is the ray field affected by caustics and anticaustics associated with the singularity?

## II. RAY TRACING IN ANISOTROPIC MEDIA WITH SINGULARITIES

Ray-tracing equations for inhomogeneous anisotropic elastic media are expressed as follows:[20,22,24]

$$\frac{dx_i}{d\tau}=a_{ijkl}p_l g_j g_k, \quad \frac{dp_i}{d\tau}=-\frac{1}{2}\frac{\partial a_{jkln}}{\partial x_i}p_k p_n g_j g_l, \qquad (1)$$

where $\mathbf{x}$ is the position vector, $\tau$ is the travel time, $\mathbf{p}=\partial\tau/\partial\mathbf{x}=\mathbf{n}/c$ is the slowness vector, $\mathbf{n}$ is the slowness direction, $c$ is the phase velocity, $\mathbf{g}$ is the polarization vector, and $a_{ijkl}$ is the density-normalized elasticity tensor. The polarization vector $\mathbf{g}$ is calculated from

$$\Gamma_{jk}g_k=Gg_j, \qquad (2)$$

where

$$\Gamma_{jk}(\mathbf{n})=a_{ijkl}n_i n_l. \qquad (3)$$

The Christoffel tensor $\Gamma_{jk}(\mathbf{n})$ has three eigenvalues $G$, which are real valued and positive ($G=c^2$), and three eigenvectors $\mathbf{g}$. The eigenvalues correspond to three waves ($P$, $S1$, and $S2$) propagating in anisotropic media, and the eigenvectors correspond to the polarization vectors of these three waves.

Equations (1) and (2) can be readily used for tracing rays outside singularities. Since the Christoffel tensor is nondegenerate, the polarization vector $\mathbf{g}$ is determined uniquely from Eq. (2) and the right-hand sides of Eq. (1) are evaluated without difficulties. However, if the medium contains singularities, Eqs. (1) and (2) are not sufficient for tracing rays. Since the Christoffel tensor is degenerate in singularities, Eq. (2) yields an ambiguous solution for $\mathbf{g}$. Hence, we cannot evaluate the right-hand sides of Eq. (1) uniquely. In this case, Eqs. (1) and (2) must be complemented by an additional condition requiring the polarization vector of the traced wave to be continuous along the ray.[24] This condition is automatically satisfied when tracing rays in regular directions, but must be explicitly required in singular directions. If we do not pose this condition, the ray tracing can produce unphysical abrupt changes of the ray direction in the singularity.

## III. EXAMPLES

The behavior of rays is studied near the kiss, conical, and wedge singularities[9,15,17] occurring in transversely isotropic, cubic, and monoclinic media. The media are chosen to be simple and illustrative rather than to describe properties of a real specific material. The geometry of rays is studied using the so-called ''ray plots.'' The ray plots are equal-area plots, which transform each ray direction into a point inside a circle (see Fig. 1). The center of the circle corresponds to the

 

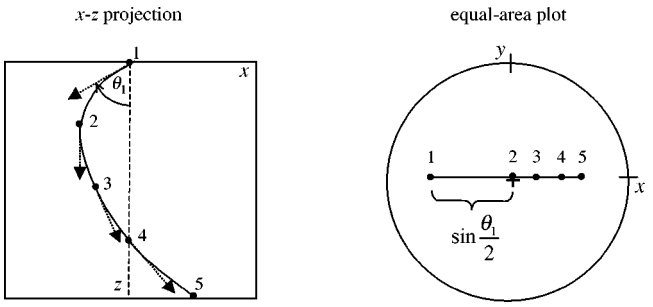


FIG. 1. The $x$-$z$ (left) and equal-area (right) projections of a ray. The center of the circle coincides with the vertical axis. The circle corresponds to a constant deviation of ray directions from the vertical axis. The dots mark the points on the ray (left) and the corresponding ray directions at these points (right).

vertical direction. The points on the circle correspond to a constant deviation of rays from the vertical axis. The position of the point is calculated from the ray direction as follows:[25]

$$x=\sin\frac{\theta}{2}\cos\phi, \quad y=\sin\frac{\theta}{2}\sin\phi, \tag{4}$$

where $\theta$ is the deviation of the ray from the vertical axis and $\phi$ is the polar angle of the ray direction defined in the horizontal plane. If the ray is a straight line, it projects onto one point in the ray plot. If the ray is bent due to a gradient in the medium, the ray projects onto a curve. The form of the curve defines the variation of the ray direction in time. The ray plots are particularly suitable for illustrating a complicated three-dimensional (3D) geometry of rays.

### A. Kiss singularity

The kiss singularity arises if the slowness sheets of two waves touch tangentially at an isolated point. A typical kiss singularity occurs along the rotational symmetry axis in transverse isotropy and along symmetry axes in cubic and tetragonal symmetries.[13,14,16,26] We consider two anisotropy models (see Fig. 2): (a) transverse isotropy and (b) cubic anisotropy. Both models are inhomogeneous with a constant velocity gradient $\epsilon$ along the $x$ axis. The source of waves is situated at the origin of coordinates. At the source the elastic parameters are (in $\mathrm{km^2\,s^{-2}}$) (a) $a_{11}=a_{22}=a_{33}=6.25$, $a_{44}=a_{55}=a_{66}=2.50$, $a_{12}=1.25$, and $a_{13}=a_{23}=4.50$ and (b) $a_{11}=a_{22}=a_{33}=6.25$, $a_{44}=a_{55}=a_{66}=2.08$, and $\gamma=a_{12}-a_{11}+2a_{44}=2.00$. The parameter $\gamma$ is the measure of the strength of anisotropy. The elastic parameters at other points of the medium are calculated as follows:

$$a_{kl}(x)=a_{kl}(x_0)(1+\epsilon x)^2, \tag{5}$$

where $a_{kl}(x_0)$ are the density-normalized elastic parameters at the source in the Voigt notation and the gradient $\epsilon$ equals $0.01\ \mathrm{km^{-1}}$. The anisotropy in both models is rather strong; hence wave sheets form triplications (see Fig. 2).

Anisotropy model (a) generates a kiss singularity along the vertical axis. The topological charge of the field of polarization vectors is $+1$ in the singularity. The shapes of the slowness and wave sheets in the singularity and its vicinity are convex for the fast $S$ wave, but concave for the slow $S$ wave. The rays are shot from the source in the following interval of angles: $\vartheta=5°$, $\varphi\in\langle -40°,40°\rangle$ in steps of 8°, where $\vartheta$ is the deviation of the slowness vector from the vertical axis and $\varphi$ is the polar angle of the slowness vector.

Figure 3 shows the ray plots for fast and slow $S$ waves near the kiss singularity in model (a). The gradient in the medium is along the $x$ axis and causes that rays are not straight lines, but change their directions with time. The change of the ray directions follows the direction of the gradient in the medium for both $S$ waves, but the sign of this change is opposite. This is caused by the different shapes of the slowness sheets near the singularity: the slowness sheet is convex for the fast $S$ wave, but concave for the slow $S$ wave. No other irregularities are observed in the ray field. Hence, one can conclude that the ray field is fully controlled by the gradient in the medium and that the kiss singularity induces no effects or anomalies in the ray field.

Also anisotropy model (b) generates a kiss singularity along the vertical axis. The topological charge of the polarization field is $+1$ in the singularity. The shapes of the slowness and wave sheets are more complex in model (b) than in model (a). The slowness and wave sheets are not smooth and the Gaussian curvature is not defined in the singularity. Moreover, the singularity is touched by caustics on the wave surface (see Fig. 4, upper plots). The rays are shot from the source in the following interval of angles: $\vartheta=16°$, $\varphi\in\langle -35°,35°\rangle$ in steps of 5°.

The behavior of the rays near the singularity is rather complex (see Fig. 4, lower plots). The rays do not follow the direction of the velocity gradient in the medium as in model (a), but they can deviate significantly from this direction, forming complicated 3D curves. The ray field is also affected by the caustics occurring around the singularity and touching the singularity.

### B. Conical singularity

The conical singularity arises if two slowness sheets touch through vertices of cone-shaped surfaces.[9,27,28] The singularity on the slowness surface generates a caustic and anticaustic on the wave surface.[14,15,17,29] The anticaustic is circular or elliptical.

The behavior of rays near a conical singularity is studied in two anisotropic models (see Fig. 5): (c) transverse isotropy and (d) cubic anisotropy. Both models are inhomogeneous with constant velocity gradient $\epsilon=0.01\ \mathrm{km^{-1}}$ along the $x$ axis. The source of waves is situated at the origin of the coordinates. At the source the elastic parameters are (in $\mathrm{km^2\,s^{-2}}$) (c) $a_{11}=a_{22}=a_{33}=6.00$, $a_{44}=a_{55}=a_{66}=3.00$, $a_{12}=a_{11}-2a_{66}=0$, and $a_{13}=a_{23}=0$ and (d) $a_{11}=a_{22}=a_{33}=6.25$, $a_{44}=a_{55}=a_{66}=2.08$, and $\gamma=a_{12}-a_{11}+2a_{44}=2.50$. The elastic parameters at other points of the medium were calculated using Eq. (5).

Anisotropy (c) is a transverse isotropy with a vertical symmetry axis (see Fig. 5, upper plots). This transverse isotropy is, however, very special, because it forms a conical singularity along the symmetry axis,[30] instead of the kiss singularity usually observed under this symmetry. The topo-

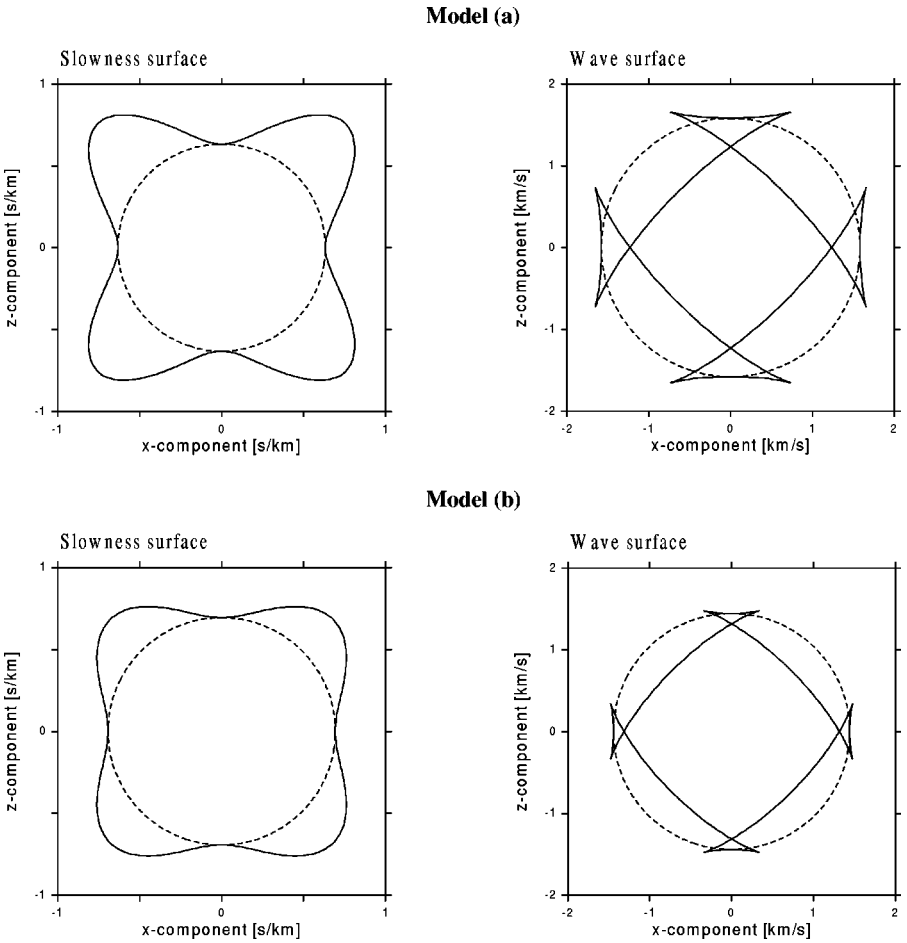


FIG. 2. The sections of the slowness and wave surfaces for anisotropic models (a) and (b) in the $x$-$z$ plane. The dashed and solid lines denote the slowness and wave sheets of the fast and slow waves, respectively. For the parameters of the (a) and (b) models, see the text.

logical charge of the polarization field in the singularity is $+1$. The conical singularity generates a caustic and an anticaustic. The caustic is along the symmetry axis. The anticaustic is circular deviating from the symmetry axis by angle $\theta = 26.56°$. The rays are shot from the source in the following interval of angles: $\vartheta = 15°$, $\varphi \in \langle -50°,\ 50° \rangle$ in steps of 10°, where $\vartheta$ is the deviation of the slowness vector from the vertical axis and $\varphi$ is the polar angle of the slowness vector.

The ray field near the conical singularity is shown in Fig. 6. The ray field is mainly controlled by the anticaustic associated with the conical singularity. The anticaustic distorts the rays and causes that the rays cannot touch it. Hence the anticaustic behaves like an obstacle, which must be bypassed. The only rays touching and crossing the anticaustic are rays lying in the $x$-$z$ plane. If the ray crosses the anticaustic, the fast wave becomes slow and the slow wave becomes fast. If the ray deviates from the $x$-$z$ plane and approaches the anticaustic, it cannot cross the singularity and is bent (see Fig. 6, lower plots). Hence, the anticaustic separates two domains: the domain of the fast wave that is outside the anticaustic and the domain of the slow wave that is inside the anticaustic. The rays of the slow wave are captured inside the anticaustic. They are prevented from crossing the anticaustic and focused into the point caustic, which is in the center of the anticaustic. Thus the caustic focuses rays while the anticaustic repels them.

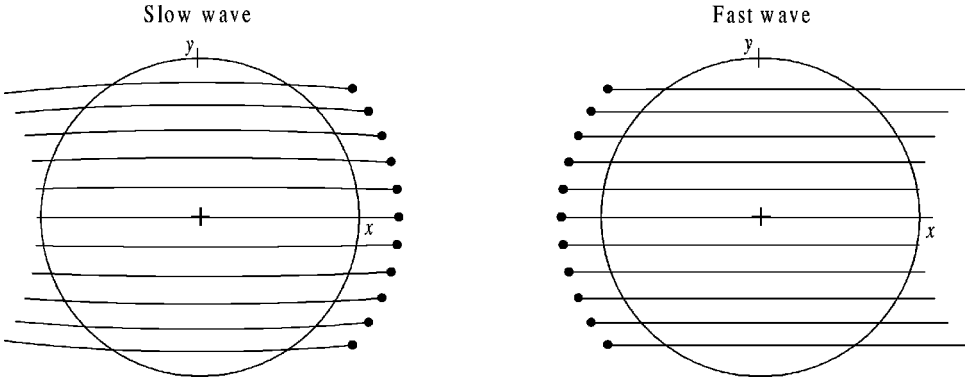


FIG. 3. The behavior of rays near the kiss singularity in model (a). The cross marks the kiss singularity. The left (right) circle corresponds to deviations of 10° (4°) of the ray directions from the singularity. The dots mark the initial directions of the rays.

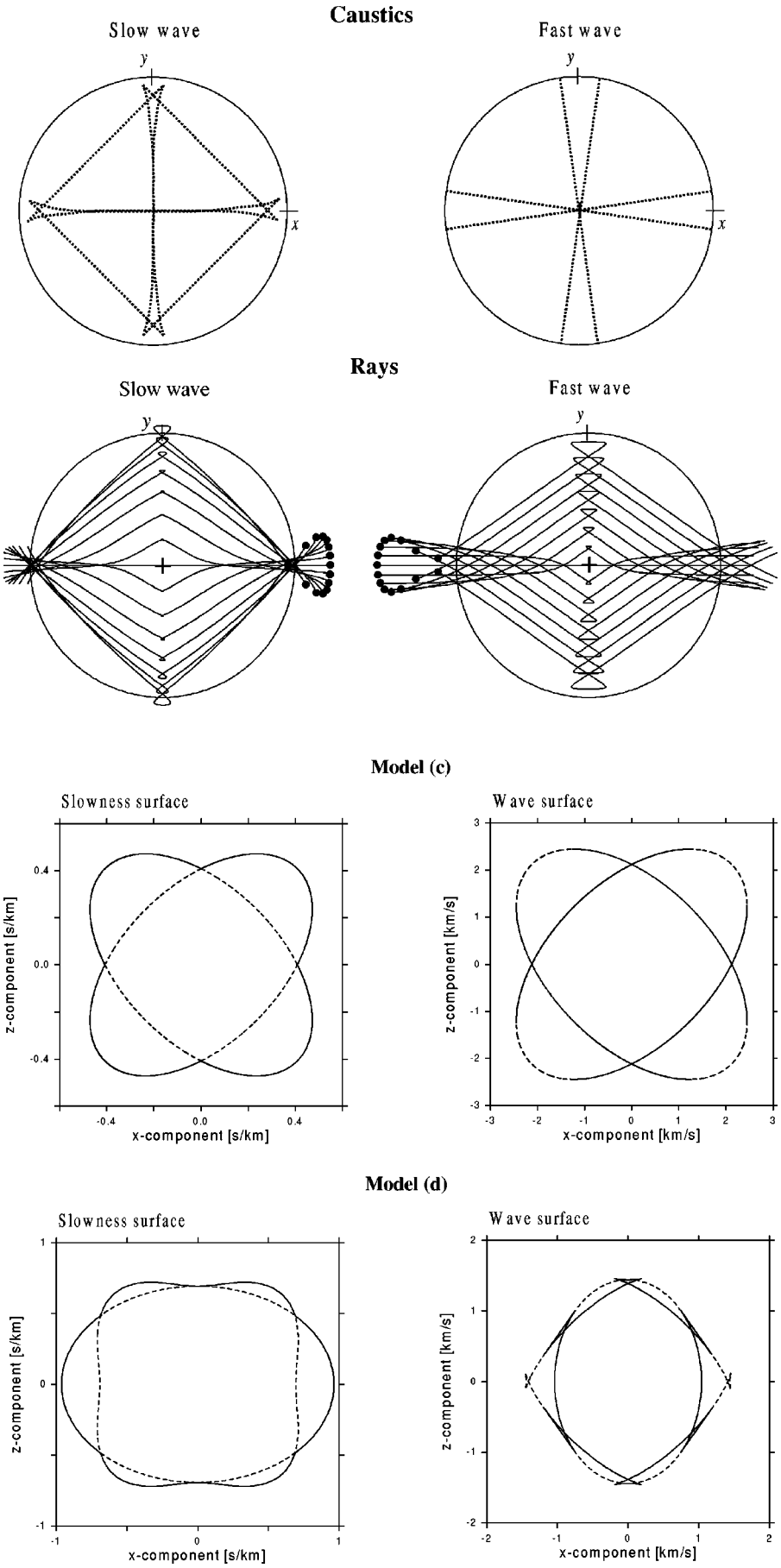


FIG. 4. The form of caustics (upper plots, dotted lines) and of rays (lower plots, solid lines) near the kiss singularity in model (b). The plots are centered on the singularity. The circles correspond to a deviation of 13° of the ray directions from the singularity. The dots in the lower plots mark the initial directions of the rays.

FIG. 5. The sections of the slowness and wave surfaces for anisotropic models (c) and (d) in the $x$-$z$ plane. The dashed and solid lines denote the slowness and wave sheets of the fast and slow waves, respectively. The $x$ axis in model (d) is along the $\langle 110 \rangle$ crystallographic axis. For the parameters of the (c) and (d) models, see the text.

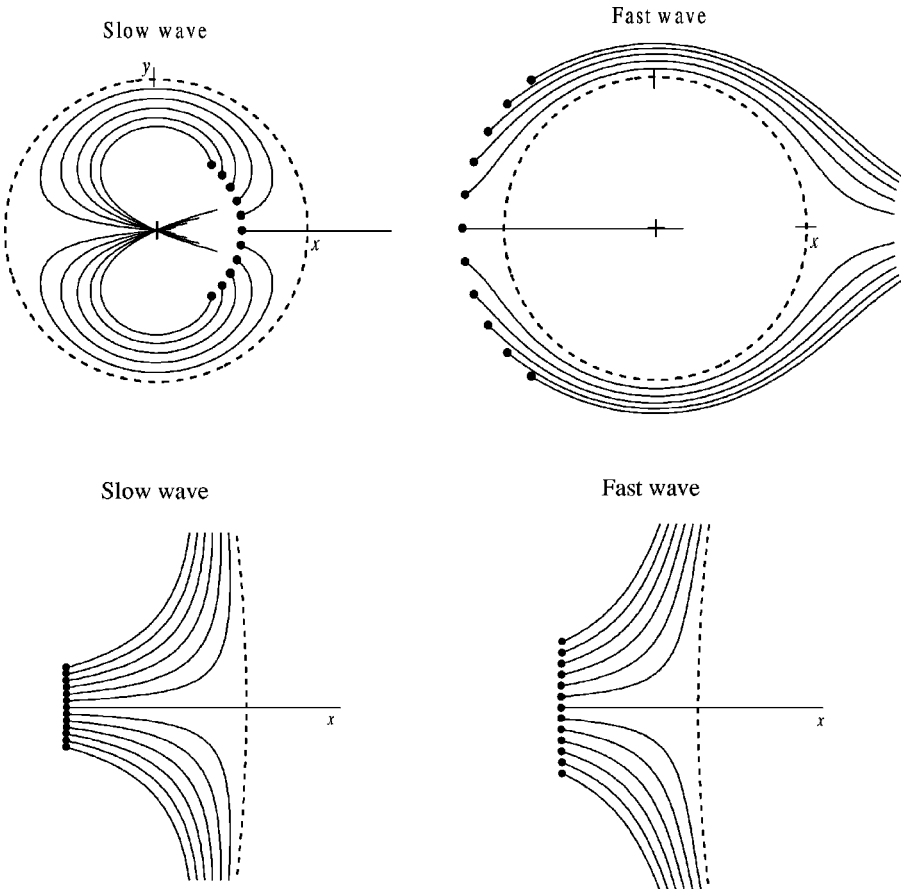


FIG. 6. The ray plots for the fast (right) and slow (left) waves near the conical singularity in model (c). The anticaustic (dashed line) corresponds to a deviation of 26.56° of the ray directions from the vertical axis. The dots mark the initial directions of the rays. The lower plots show the detailed behavior of the rays in the close vicinity of the anticaustic.

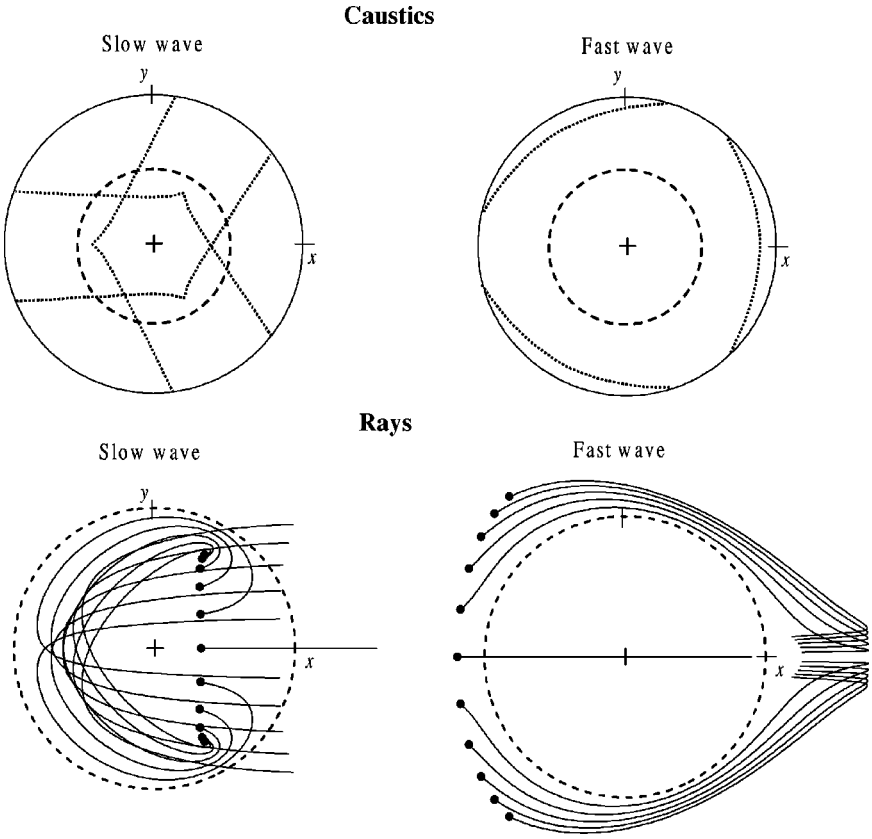


FIG. 7. The form of caustics (upper plots, dotted lines) and of rays (lower plots, solid lines) near the conical singularity in model (d). The plots are centered on the singularity. The anticaustics (dashed circles) correspond to a deviation of 25.30° of the ray directions from the vertical axis. The boundary circles in the upper plots correspond to a deviation of 50° of the ray directions from the vertical axis. The scales of upper and lower figures are different.

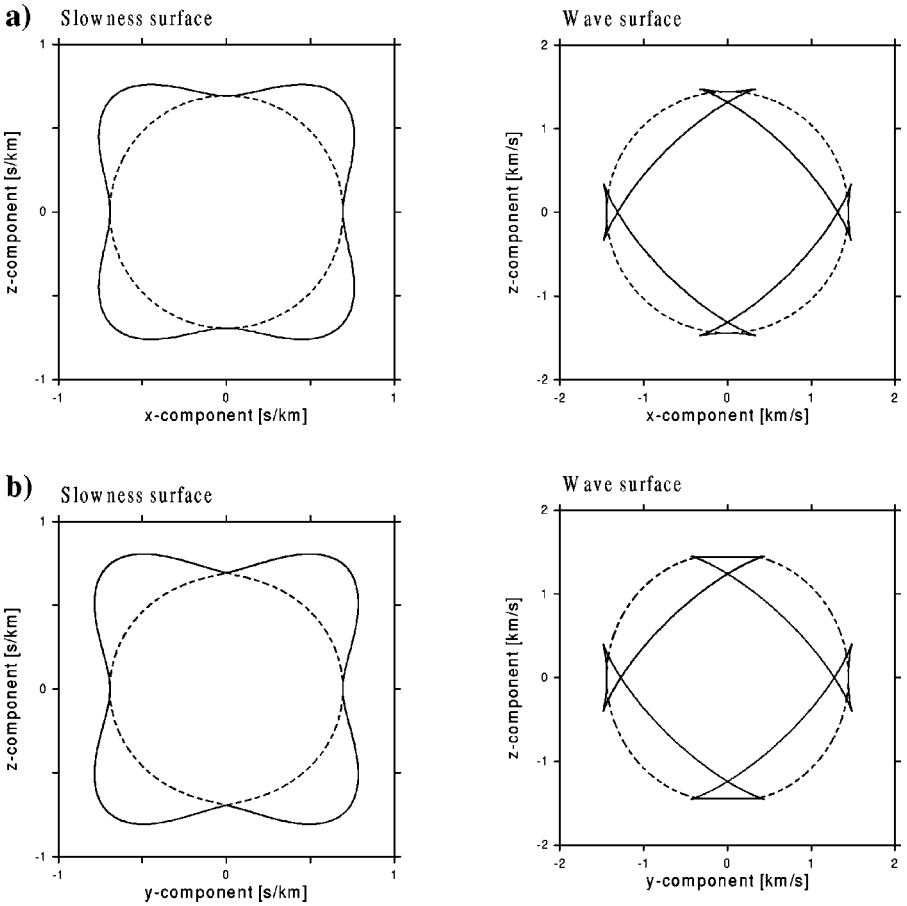


FIG. 8. The sections of the slowness and wave surfaces for monoclinic anisotropy in the *x*-*z* (a) and *y*-*z* (b) planes. The dashed and solid lines denote the slowness and wave sheets of the fast and slow waves, respectively. For the parameters of the model, see the text.

Anisotropy (d) generates a conical singularity in the $\langle 111 \rangle$ direction. The topological charge of the polarization field in the singularity is 0.5. The anisotropy is rotated so that the singularity is along the *z* axis. The singularity generates a circular anticaustic. The ray directions at the anticaustic deviate from its center by angle $\theta = 25.30°$. The anisotropy also forms caustics for both *S* waves (see Fig. 7, upper plots). The rays were shot from the source in the following interval of angles: $\vartheta = 6°$, $\varphi \in \langle -50°,\ 50° \rangle$ in steps of 10°.

Figure 7 (lower plots) shows ray plots for both *S* waves. The geometry of rays is affected by caustics and anticaustics near the singularity. Likewise in model (c) (see Fig. 6), the anticaustic represents a barrier for rays. The rays of the fast *S* wave flow around the anticaustic, while the rays of the slow *S* wave are captured inside the anticaustic. The captured rays pass the caustic, which is generated by the conical singularity. Passing the caustic the rays leave the anticaustic domain, and the influence of the anticaustic on the rays is lost.

### C. Wedge singularity

The wedge singularity is defined as the direction in which two slowness sheets touch through the vertices of wedge-shaped surfaces.[9,31] The wedge singularity arises from the conical singularity, if one of the semiaxes of the elliptical base of the cone goes to infinity. The wedge singularity generates a linear anticaustic on the wave surface. Since the wedge singularity is always touched by parabolic lines on the slowness sheet of the slow wave, the anticaustic is touched by the caustic at two points on the wave surface.

The ray field near the wedge singularity is studied in monoclinic anisotropy (see Fig. 8) built by perturbing a cubic anisotropy by adding nonzero parameter $a_{25}$. The anisotropy model is inhomogeneous with constant velocity gradient $\epsilon = 0.01\ \mathrm{km}^{-1}$ along the *x* axis. The source of waves is situated at the origin of coordinates. At the source the elastic parameters are (in $\mathrm{km}^2\,\mathrm{s}^{-2}$) $a_{11} = a_{22} = a_{33} = 6.25$, $a_{44} = a_{55} = a_{66} = 2.08$, $\gamma = a_{12} - a_{11} + 2a_{44} = 2.00$, and $a_{25} = 1.00$. The remaining parameters are zero. The elastic parameters at other points of the medium were calculated using Eq. (5).

The studied anisotropy generates the wedge singularity along the vertical axis. The topological charge of the polarization field in the singularity is 0. The shapes of the slowness and wave sheets illustrate the very exceptional properties of the wedge singularity (see Fig. 8). While the slowness sheets of *S* waves touch tangentially in the *x*-*z* plane, they touch through the vertices of two wedges in the *y*-*z* plane. The linear anticaustic associated with the singularity is along the *y* axis. The anticaustic is touched at its edges by caustics (see Fig. 9, upper plots). The rays were shot from the source in the following interval of angles: $\vartheta = 10°$, $\varphi \in \langle -5°, 5° \rangle$ in steps of 1°.

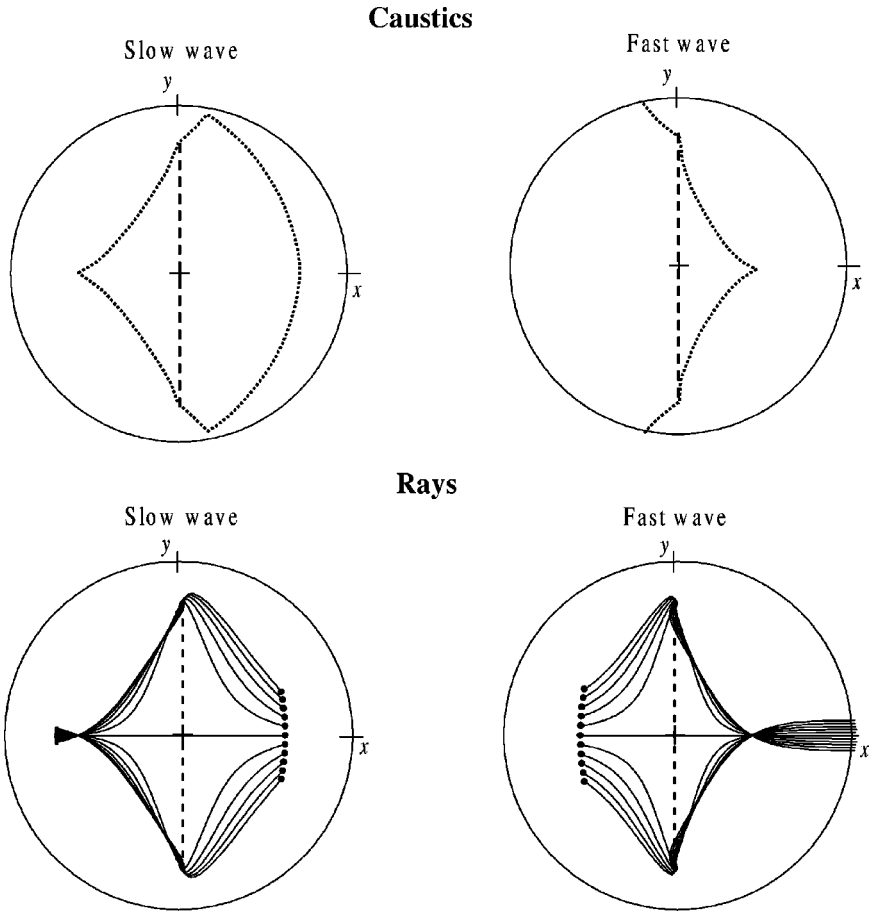


FIG. 9. Caustics on the wave sheets (upper plots, dotted lines) and rays (lower plots, solid lines) for the fast (right) and slow (left) *S* waves near the wedge singularity. The dashed line marks the anticaustic associated with the wedge singularity. The boundary circles correspond to a deviation of 18° of the ray directions from the vertical axis.

The ray plots (see Fig. 9, lower plots) show that the geometry of rays is strongly affected by the presence of an anticaustic. Similarly as for the conical singularity, the anticaustic prevents rays from simply following the gradient direction and deflects them so that they do not cross but move around the anticaustic. The rays are bent and focused at the edges of the anticaustic, where the anticaustic is touched by the caustic. Beyond the anticaustic, the rays are forced to pass a cusped edge of the anticaustic, which lies in the *x*-*z* plane. The only rays not affected by the anticaustic are the rays in the *x*-*z* plane.

## IV. CONCLUSIONS

The geometry of rays can display a complicated pattern in inhomogeneous anisotropic media. The ray field is affected not only by the velocity gradient as in isotropic media, but also by the symmetry and strength of anisotropy. The anisotropy can strongly affect the ray fields and introduce effects, which cannot be observed under isotropy. For example, while the rays are 2D (planar) curves in 1D inhomogeneous isotropic media, the rays can form complicated 3D curves in 1D inhomogeneous anisotropic media. While the bending of rays follows the direction of the velocity gradient in isotropic media, the bending of rays may significantly deviate from this direction in anisotropic media.

Peculiarities in the ray fields can also be induced by singularities in anisotropy. This concerns namely conical and wedge singularities, which generate caustics and anticaustics in their vicinity. The role of the anticaustic in forming the ray field is particularly interesting. The anticaustic prevents the rays from simply following the gradient direction in the medium and deflects them so that they do not cross it. Hence, the anticaustic behaves like a barrier for a ray. The anticaustic of the wedge singularity is linear and the rays move around it. The anticaustic of the conical singularity is elliptical or circular and separates two domains: the domain of the fast wave that is outside the anticaustic and the domain of the slow wave that is inside the anticaustic. The rays outside the anticaustic move around it, while the rays inside the anticaustic are captured. The captured rays are forced to pass the caustic generated by the conical singularity. Passing the caustic the influence of the anticaustic on the rays is lost. One can observe that the anticaustic is also crossed by a ray, but only in very exceptional cases. If the ray passes the anticaustic, the slow wave becomes fast and the fast wave becomes slow.

## ACKNOWLEDGMENTS

I thank V. Červený for stimulating discussions on the subjects. This work was supported by the Grant Agency of the Czech Republic, Grant No. 205/00/1350, and by the Consortium project ''Seismic waves in complex 3-D structures (SW3D).''

*Electronic address: vv@ig.cas.cz

[1] F. I. Fedorov, *Theory of Elastic Waves in Crystals* (Plenum, New York, 1968).
[2] M. J. P. Musgrave, *Crystal Acoustics* (Holden-Day, San Francisco, 1970).
[3] S. Crampin and M. Yedlin, J. Geophys. **49**, 43 (1981).
[4] M. J. P. Musgrave, Proc. R. Soc. London, Ser. A **401**, 131 (1985).
[5] B. M. Darinskii, Crystallogr. Rep. **39**, 697 (1994).
[6] Ph. Boulanger and M. Hayes, Proc. R. Soc. London, Ser. A **454**, 2323 (1998).
[7] K. Helbig, *Foundations of Anisotropy for Exploration Seismics* (Pergamon, New York, 1994).
[8] V. I. Alshits, A. V. Sarychev, and A. L. Shuvalov, Sov. Phys. JETP **62**, 531 (1985).
[9] A. L. Shuvalov, Proc. R. Soc. London, Ser. A **454**, 2911 (1998).
[10] V. Yu. Grechka and I. R. Obolentseva, Geophys. J. Int. **115**, 609 (1993).
[11] A. L. Shuvalov and A. G. Every, J. Acoust. Soc. Am. **101**, 2381 (1997).
[12] A. L. Shuvalov and A. G. Every, Phys. Rev. B **53**, 14 906 (1996).
[13] V. Vavryčuk, Stud. Geophys. Geod. **46**, 249 (2002).
[14] D. C. Hurley and J. P. Wolfe, Phys. Rev. B **32**, 2568 (1985).
[15] A. G. Every, Phys. Rev. B **34**, 2852 (1986).
[16] A. G. Every, Phys. Rev. B **37**, 9964 (1988).
[17] J. P. Wolfe, *Imaging Phonons. Acoustic Wave Propagation in Solids* (Cambridge University Press, Cambridge, England, 1998).
[18] V. Červený, Geophys. J. R. Astron. Soc. **29**, 1 (1972).
[19] V. Červený, I. A. Molotkov, and I. Pšenčík, *Ray Method in Seismology* (Charles University Press, Praha, Czech Republic, 1977).
[20] D. Gajewski and I. Pšenčík, Geophys. J. R. Astron. Soc. **91**, 383 (1987).
[21] D. Gajewski and I. Pšenčík, J. Geophys. Res. **95**, 11 301 (1990).
[22] V. Červený, *Seismic Ray Theory* (Cambridge University Press, Cambridge, England, 2001).
[23] I. Pšenčík and J. Dellinger, Geophysics **66**, 308 (2001).
[24] V. Vavryčuk, Geophys. J. Int. **145**, 265 (2001).
[25] K. Aki and P. G. Richards, *Quantitative Seismology* (University Science Books, Sausalito, California, 2002), p. 105.
[26] V. Vavryčuk, Geophys. J. Int. **138**, 581 (1999).
[27] R. Burridge, Q. J. Mech. Appl. Math. **20**, 41 (1967).
[28] G. Rümpker and C. J. Thomson, Geophys. J. Int. **118**, 759 (1994).
[29] D. C. Hurley, M. T. Ramsbey, and J. P. Wolfe, in *Phonon Scattering in Condensed Matter V*, edited by A. C. Anderson and J. P. Wolfe (Springer, New York, 1986).
[30] R. G. Payton, Q. J. Mech. Appl. Math. **45**, 183 (1992).
[31] V. Vavryčuk, Geophys. J. Int. **152**, 318 (2003).